THE JOURNAL OF PHYSICAL CHEMISTRY B

Article

pubs.acs.org/JPCB

Critical Slowing of Density Fluctuations Approaching the Isotropic–Nematic Transition in Liquid Crystals: 2D IR Measurements and Mode Coupling Theory

Kathleen P. Sokolowsky, Heather E. Bailey, David J. Hoffman, Hans C. Andersen, and Michael D. Fayer*

Department of Chemistry, Stanford University, Stanford, California 94305, United States

ABSTRACT: Two-dimensional infrared (2D IR) data are presented for a vibrational probe in three nematogens: 4-cyano-4′-pentylbiphenyl, 4-cyano-4′-octylbiphenyl, and 4-(*trans*-4-amylcyclohexyl)-benzonitrile. The spectral diffusion time constants in all three liquids in the isotropic phase are proportional to $[T^*/(T - T^*)]^{1/2}$, where T^* is 0.5−1 K below the isotropic–nematic phase transition temperature (T_{NI}). Rescaling to a reduced temperature shows that the decays of the frequency–frequency correlation function (FFCF) for all three nematogens fall on the same curve, suggesting a universal dynamic behavior of nematogens above T_{NI}. Spectral diffusion is complete before significant orientational relaxation in the liquid, as measured by optically heterodyne detected-optical Kerr effect (OHD-OKE) spectroscopy, and before any significant orientational randomization of the probe measured by polarization selective IR pump–probe experiments. To interpret the OHD-OKE and FFCF data, we constructed a mode coupling theory (MCT) schematic model for the relationships among three correlation functions: ϕ_1, a correlator for large wave vector density fluctuations; ϕ_2, the orientational correlation function whose time derivative is the observable in the OHD-OKE experiment; and ϕ_3, the FFCF for the 2D IR experiment. The equations for ϕ_1 and ϕ_2 match those in the previous MCT schematic model for nematogens, and ϕ_3 is coupled to the first two correlators in a straightforward manner. Resulting models fit the data very well. Across liquid crystals, the temperature dependences of the coupling constants show consistent, nonmonotonic behavior. A remarkable change in coupling occurs at ∼5 K above T_{NI}, precisely where the rate of spectral diffusion in 5CB was observed to deviate from that of a similar nonmesogenic liquid.

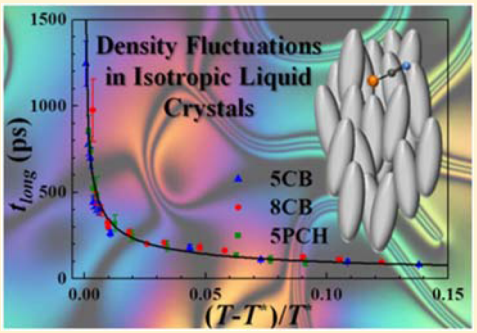

I. INTRODUCTION

The dynamics of nematic liquid crystals in the isotropic phase have drawn substantial attention for decades due to the distinctive pretransitional effects that appear as the isotropic to nematic phase transition is approached from above. Regions of nematic order, referred to as pseudonematic domains, persist even tens of degrees above the isotropic–nematic phase transition temperature (T_{NI}).[1] Landau–de Gennes theory was developed in part to describe these pseudonematic domains. The temperature dependence of the orientational correlation length, ξ, of the pseudonematic domains is given by

$$\xi(T) = \xi_0\left(\frac{T^*}{T - T^*}\right)^{1/2}, \quad T > T^* \tag{1}$$

where ξ_0 is a molecular length scale (4–8 Å) and T^* is the critical temperature (typically 0.5–1 K below T_{NI}).[1−4] The complete orientational relaxation of a nematic liquid crystal in the isotropic phase requires the complete randomization of these domains. Thus, the divergence in the size of pseudonematic domains is paralleled by divergence in the orientational relaxation time, τ_{LdG}. Landau–de Gennes theory gives

$$\tau_{LdG} = \frac{V_{eff}^*\eta(T)}{k_B(T - T^*)} \tag{2}$$

where $\eta(T)$ is the viscosity, V_{eff}^* is the effective volume, and k_B is the Boltzmann constant.[1] Landau–de Gennes theory has been confirmed by a number of both time and frequency domain experiments such as depolarized light scattering, dynamic light scattering, magnetic and electric birefringence, dielectric relaxation, and optical Kerr effect spectroscopy.[5−14]

Optically heterodyne detected-optical Kerr effect (OHD-OKE) spectroscopy reports the time derivative of the polarizability–polarizability correlation function. This correlation function is equivalent to the collective orientational correlation function at all but very short times, during which there can also be collision induced contributions.[15,16] OHD-OKE has been used to characterize the orientational dynamics of pseudonematic domains up to ∼50 K above T_{NI} when the size of the domain becomes similar to the molecular volume.[9−13,17] Prior to the final exponential decay of the correlation function, related to the complete randomization of pseudonematic domains, multiple fast nonexponential decays

Received: May 17, 2016
Revised: June 29, 2016
Published: July 1, 2016

DOI: 10.1021/acs.jpcb.6b04997
J. Phys. Chem. B 2016, 120, 7003−7015

are observed. The nonexponential decay of the correlation function is typically attributed to cage fluctuations that take place on shorter time scales than rotational diffusive motion.

The nonexponential and final Landau−de Gennes exponential decay of the collective correlation function for a system with pseudonematic domains can be described with the modified mode coupling theory (MCT) schematic model of Li et al.[17] This model describes the time dependence of two correlation functions, a large wave vector density fluctuation correlator (ϕ_1) and a collective orientational correlator (ϕ_2).[18,19] It takes into account the divergent behavior approaching T_{NI} for nematogens as well as the influence of slowly relaxing, large wave vector density fluctuations on the dynamics.[20] The parameters of the model can be adjusted so that the time derivative of ϕ_2 fits the OHD-OKE data. The fitting process also yields the time dependence of ϕ_1.

Although the collective orientational relaxation dynamics measured with OHD-OKE have been well characterized for nematogens in the isotropic phase, the influence of pseudonematic domains on the dynamics of individual molecules remains obscure. Introduction of probes into liquid crystal systems proves problematic, as small amounts of impurities can change the liquid crystal dynamics of interest.[21,22] It has been shown previously that in low concentration a small vibrational probe on a molecule possessing a similar structure to the nematogen can be used, without significantly perturbing the properties of the liquid, to interrogate the dynamics using two-dimensional infrared (2D IR) vibrational echo experiments.[23−25] Thus, the combination of OHD-OKE and 2D IR spectroscopies provides dynamical information on a wide range of molecular motions on various time scales in isotropic phase liquid crystal systems.

2D IR experiments have previously been conducted on the CN stretch of the SeCN moiety of 4-pentyl-4′-selenocyanobiphenyl (5SeCB) in the nematic liquid crystal 4-cyano-4′-pentylbiphenyl (5CB).[24] The absorption band of the CN stretch is inhomogeneously broadened due to the range of structural environments that exist at any moment of time. As the liquid structure experienced by the vibrational probe evolves, the oscillator frequency changes (spectral diffusion), moving throughout the line shape. 2D IR spectroscopy quantifies spectral diffusion, providing a direct link to the structural fluctuations of the system.

To study the influence of pseudonematic domains on spectral diffusion, studies on 5SeCB in 5CB were compared to those of 4-pentyl-4′-thiocyanobiphenyl (5SCB) in 4-pentylbiphenyl (5B).[23,24] 5B is extremely similar in molecular structure to 5CB, only lacking the nitrile group; it does not display liquid crystal behavior. Well above T_{NI} for 5CB, the spectral diffusion in both the 5CB nematogen and the 5B normal liquid were strikingly similar. The time constants associated with frequency fluctuations were found to be identical within experimental error. However, the dynamics reported on by spectral diffusion differed dramatically within 5 K of T_{NI}. While the slowing of dynamics in 5B tracked the viscosity as the sample was cooled, in the liquid crystal 5CB, the time constants for spectral diffusion were found to diverge. The divergence of the time constants fits the form $t = A|T - x_c|^p$. Within experimental error, $x_c = T^*$ and $p = -1/2$ for all of the time constants. The data could then be represented by

$$t = a\left(\frac{T^*}{T - T^*}\right)^{1/2}, \quad T > T^* \tag{3}$$

exactly the same form as given for the correlation length, ξ, of pseudonematic domains in eq 1.[24]

While the time scale for spectral diffusion was observed to be closely tied to the existence of pseudonematic domains, domain orientational relaxation can be ruled out as the source of spectral diffusion.[24] Not only is spectral diffusion much faster than the complete orientational relaxation of domains measured with OHD-OKE spectroscopy, but the spectral diffusion is essentially complete within the experimental window of 2D IR (∼1 ns) at even the coldest temperature, at which the orientational relaxation is on the μs time scale. The large wave vector density correlation function calculated from an MCT schematic model fit to the OHD-OKE data is much closer in time scale to the spectral diffusion observed.[23,24] While this large wave vector density correlation function decays on the appropriate time scale, it does not have the functional form or temperature dependence seen in the spectral diffusion data.

In the present paper, we confirm the divergence of the spectral diffusion in two more liquid crystal systems, 4-cyano-4′-octylbiphenyl (8CB) and 4-(trans-4-amylcyclohexyl)-benzonitrile (5PCH). The spectral diffusion of all three isotropic phase liquid crystals have the same functional form of the temperature dependence of the divergence as T_{NI} is approached from above. An MCT schematic model is given that describes both the spectral diffusion data obtained from 2D IR experiments and the orientational relaxation data obtained from OHD-OKE experiments for the nematogens in the isotropic phase.[17]

II. EXPERIMENTAL METHODS

II.A. Sample Preparation. 5PCH was purchased from TCI America; 8CB was purchased from Sigma-Aldrich. Both chemicals were used as received without additional purification. 5SeCB was synthesized in a two-step procedure from 4-bromo-4′-pentylbiphenyl as previously described.[24] Solutions of 2.5 mol % 5SeCB in 8CB and 5PCH were passed through 0.02 μm filters (Anotop) before loading in experimental sample cells. No change in the optical density of the 5SeCB nitrile stretch was observed after filtration; thus, complete dissolution of the probe molecule was achieved in both liquid crystals.

For OHD-OKE experiments, the liquid crystal solution was contained between two 3 mm thick CaF_2 windows, mounted in a custom cell with 1 cm path length. For all infrared spectroscopy, the sample was sandwiched between two 3 mm thick CaF_2 windows separated by a 250 μm (5PCH) or 390 μm (8CB) Teflon spacer. The windows were held in a copper sample cell. Temperature dependent studies were conducted from roughly 311 to 355 K, maintained within 0.1 K with a PID temperature controller.

II.B. OHD-OKE Spectroscopy. The details of the OHD-OKE spectroscopy setup employed have been described in detail elsewhere.[26] Briefly, a Ti:sapphire oscillator/regenerative amplifier creates pulses with a power up to 300 μJ/pulse with pulse widths varying from 60 fs to 125 ps at a 5.4 kHz repetition rate. The output beam then is split to create a pump and a probe beam.

OKE is a nonresonant pump−probe spectroscopy in which a linearly polarized pump pulse induces a transient birefringence in a sample that is then interrogated at a later time by a probe pulse polarized at 45° relative to the pump. The amount of birefringence remaining at the delayed arrival of the probe is related to the orientational relaxation of the sample. Persisting birefringence will cause an ellipticity in the probe pulse, which

DOI: 10.1021/acs.jpcb.6b04997
J. Phys. Chem. B 2016, 120, 7003−7015

can be measured after a crossed polarizer.[27,28] The signal decays in time as the birefringence is reduced through orientational relaxation; the signal is the time derivative of the polarizability−polarizability correlation function, which is the same as the derivative of the orientational correlation function at all but very short times.[15,16]

Optical heterodyne detection is achieved by beginning with a slight ellipticity in the probe beam prior to interaction with the sample. Heterodyne detection improves the signal-to-noise ratio and permits a four shot sequence in which the probe heterodyne field is phase cycled and the pump polarization is cycled.[26,29] Data are collected with a balanced detector and lock-in amplifier from hundreds of femtoseconds to microseconds. To collect the longest time data, the physically delayed probe pulse is replaced with a CW probe beam, and the data are recorded with a 1 ns digitizer.

OHD-OKE data were collected for 2.5 mol % solutions of 5SeCB in both 5PCH and 8CB. Each decay was fit with the phenomenological function

$$F(t) = [pt^{-z} + dt^{b-1}]e^{-t/\tau} \quad (4)$$

which has been used to fit OHD-OKE data for a variety of liquids including liquid crystals.[12,13,30−34] The form of eq 4 is based on schematic MCT to account for early time non-Markovian caged dynamics and final exponential decay, which is the complete orientational randomization.[12,13,32] The first power law is the "intermediate" power law, and the second power law is the "von Schweidler" power law. For nematic liquid crystals in the isotropic phase, this final decay is the Landau−de Gennes decay involving complete randomization of pseudonematic domains.[13] A global fit of the entire data using eq 4 must be performed to obtain an accurate value of this important final exponential decay value. Data were fit from 2.5 ps to near the end of the exponential decay at all temperatures studied. As was previously observed, the exponents of the power laws were found to be temperature independent.[13,17,23,24]

II.C. Ultrafast Infrared Spectroscopy. The ultrafast IR experiments presented here employ methods and a laser setup that have been described in detail elsewhere, but a brief summary follows.[35,36] A Ti:sapphire oscillator and regenerative amplifier produce ultrafast pulses at 800 nm to pump an optical parametric amplifier (OPA). The OPA converts the light into the mid-IR (4.6 μm), resulting in an energy of ∼6 μJ/pulse at a 1 kHz repetition rate. The pulses were approximately 125 fs in duration with a bandwidth of 90 cm^{-1} full width at half-maximum. Generated mid-IR light was split into four beams for vibrational echo spectroscopy. Precision interferometry was achieved with delay stages, which controlled pulse arrival at the sample to an accuracy of <0.1 fs. An experimental window of potentially 2 ns was provided with a long delay stage.

Three of the mid-IR excitation pulses are crossed in the sample. The significantly weaker fourth pulse acts as the local oscillator (LO). Timing of the arrival of each of the three excitations pulses is set though physical delay of the computer controlled stages. The time between pulses 1 and 2, τ, is a coherence period; the time between pulses 2 and 3, T_w, is the population period, the waiting time during which dynamics of interest occur. Interaction between these three pulses and the sample generates a vibrational echo signal at a time $\leq\tau$ after pulse 3. Heterodyne detection of the signal is achieved by overlapping the LO spatially with the vibrational echo. The combined echo/LO is frequency resolved by a monochromator, which acts as a spectrograph, and detected by a 32-element mercury−cadmium−telluride detector. Dispersion by the monochromator temporally broadens the echo and LO to ∼100 ps so that they overlap in time. Heterodyne detection provides amplification of the signal and phase information through the interference of the echo with the LO. At each T_w, τ is scanned and the echo pulse moves in time relative to the LO generating a temporal interferogram at each detected frequency. The dispersion by the monochromator experimentally performs one of the two Fourier transforms to give the vertical, ω_m, axis of the 2D IR spectrum. The horizontal axis, ω_τ, is generated by numerically Fourier transforming the interferogram collected at each ω_m. Data were collected at T_w's ranging from 1 ps to 1 ns.

The dynamical details of interest are contained in the change in shape of the 2D IR spectrum as a function of T_w. This shape evolution is a reporter of spectral diffusion; a qualitative explanation of spectral diffusion follows.[35,37,38] The frequency of an individual nitrile stretch is a narrow Lorentzian due to homogeneous broadening. The center frequency is determined by the coupling of the liquid structure to the probe vibration. A Gaussian distribution of center frequencies exists for the collection of CN transitions, giving rise to inhomogeneous broadening. The total absorption line in FT-IR is given by the convolution of these Lorentzian and Gaussian profiles. The frequency of a particular oscillator in solution will evolve in time as the liquid structure changes, i.e., spectral diffusion. At long waiting times, the probe will experience all liquid structures; therefore, it will sample all frequencies in the inhomogeneous line.

The three-pulse sequence employed in vibrational echo experiments reports on the initial and final frequencies of the vibrational oscillators, separated by a population time, T_w, during which the liquid structure evolves. The initial nitrile oscillator frequencies are effectively labeled by pulses 1 and 2. The arrival of pulse 3 ends the population period and induces the emission of the vibrational echo signal. The echo signal encodes the final frequencies of the vibrational probe molecules. At short waiting times, the liquid has had little time to change. Thus, the final frequencies reported by the echo signal will differ very little from the starting frequencies. However, at long T_w, the liquid structures interacting with each probe have time to evolve. The final frequencies encoded by the echo are less correlated with the initial frequencies. The loss of correlation between initial and final frequencies of vibrational oscillators as a function of T_w appears as a change in shape of the 2D IR spectra. When the detection (ω_m) and excitation (ω_τ) frequencies are approximately equal at short T_w, the spectrum is elongated along the diagonal. When the final frequency loses correlation, the shape of the spectrum becomes more symmetric and finally completely round when T_w is long enough for all liquid environments to be sampled. In this manner, the change in shape of the 2D IR spectra as a function of T_w reports on the structural dynamics of the liquid crystal.

A fundamental time correlation function that describes spectral diffusion is the frequency−frequency correlation function (FFCF). The FFCF is defined by

$$C(t) = \langle \delta\omega(t)\delta\omega(0)\rangle \quad (5)$$

where $\omega(t)$ is the frequency of an oscillator at time t and $\omega(0)$ is the frequency of the oscillator at time $t = 0$. The FFCF was modeled with a simplified Kubo form, given by

DOI: 10.1021/acs.jpcb.6b04997
J. Phys. Chem. B 2016, 120, 7003−7015

$$C(t) = \sum_i \Delta_i^2 \exp(-t/\tau_i) \tag{6}$$

where Δ_i and τ_i are the frequency fluctuation amplitude and time constant of the ith component.[39] A process is motionally narrowed and a source of homogeneous broadening in the absorption line if $\Delta_i\tau_i < 1$; it is then not possible to determine Δ_i and τ_i individually. The contribution of homogeneous broadening to the absorption spectrum has a pure dephasing linewidth given by $\Gamma^* = \Delta^2\tau = 1/\pi T_2^*$, where T_2^* is the pure dephasing time. The measured homogeneous time also depends on the orientational relaxation and vibrational lifetime

$$\frac{1}{T_2} = \frac{1}{T_2^*} + \frac{1}{2T_1} + \frac{1}{3T_{or}} \tag{7}$$

where T_1 and T_{or} are the vibrational lifetime and orientational relaxation time, respectively. In the liquid crystal systems with long lifetime vibrational probes and exceedingly slow orientational relaxation, T_1 and T_{or} are much longer than T_2^*, so $T_2 \approx T_2^*$. The T_w dependence of the FFCF is extracted from 2D IR spectra using the Center Line Slope (CLS) method.[40,41] The CLS function of T_w, CLS(T_w), has been shown to be equal to the normalized FFCF. At each T_w, the slope of the center line is determined, and these CLS values form CLS(T_w). The difference between the CLS value at $T_w = 0$ and 1 is related to the homogeneous linewidth. To obtain the full FFCF, the CLS(T_w) is analyzed using the linear absorption spectrum to provide the homogeneous component.[40,41]

III. A MODE COUPLING MODEL FOR ORIENTATIONAL RELAXATION AND SPECTRAL DIFFUSION

A modified MCT schematic model has previously been developed to account for the orientational dynamics of nematogens in the isotropic phase as measured by OHD-OKE spectroscopy.[17−19] The model is a set of kinetic equations for two correlation functions denoted ϕ_1 and ϕ_2. ϕ_1 is a correlation function for large wave vector density fluctuations. It is the fundamental correlation function whose decay toward zero slows down as the MCT ideal glass transition is approached from higher temperatures. ϕ_2 is an orientational correlation function whose time derivative is directly related to the experimental observable of the OHD-OKE experiments.[19] The coupled equations of motion are

$$\ddot{\phi}_1(t) + \mu_1\dot{\phi}_1(t) + \Omega_1^2\phi_1(t) + \Omega_1^2\int_0^t d\tau m_1(t-\tau)\dot{\phi}_1(\tau) = 0 \tag{8a}$$

$$\ddot{\phi}_2(t) + (\mu_2 + \Gamma)\dot{\phi}_2(t) + (\Omega_2^2 + \mu_2\Gamma)\phi_2(t) + \Omega_2^2\int_0^t d\tau m_2(t-\tau)\dot{\phi}_2(\tau) + \Omega_2^2\Gamma\int_0^t d\tau m_2(t-\tau)\phi_2(\tau) = 0 \tag{8b}$$

Ω_1 and Ω_2 are undamped molecular oscillator frequencies in the terahertz range, μ_1 and μ_2 are damping coefficients, and $\Gamma = \tau_{LdG}^{-1}$. The memory functions in these equations are

$$m_1(t) = \nu_1\phi_1(t) + \nu_2\phi_1^2(t) \tag{9a}$$

$$m_2(t) = \kappa\phi_1(t)\phi_2(t) \tag{9b}$$

where ν_1 and ν_2 are the coupling coefficients of the m_1 memory function for ϕ_1 and κ is the coupling coefficient that governs the effect of ϕ_1 on ϕ_2. The initial conditions for the second order differential equations are $\phi_1(0) = \phi_2(0) = 1$ and $\dot{\phi}_1(0) = 0$ and $\dot{\phi}_2(0) = -\Gamma$.

Equations 8a and 9a are the equations for an MCT F_{12} schematic model.[42] With appropriate values of the parameters, the model can describe the slowing down of relaxation of large wave vector density fluctuations as an MCT ideal glass transition is approached. However, in the experiments on nematogens, the temperature is well above the melting point, so the systems studied are very far from the (avoided) MCT ideal glass transition. Thus, the F_{12} schematic model is an approximate (nonsingular) model for large wave vector density fluctuations.

Equations 8b and 9b are of the form of a schematic mode coupling model for a correlator whose decay is slowed down by coupling to ϕ_1.[19] In addition, this equation has been modified to be consistent with Landau−de Gennes theory at long times by inclusion of the terms that contain Γ.

The physical meaning of these equations is that the long time relaxation of the collective orientational correlation function is determined not only by the proximity to the isotropic−nematic transition (as in the Landau−de Gennes theory) but also by large wave vector density fluctuations (as described using schematic MCT). This model can be extended to describe the correlation function that is obtained from 2D IR experiments.

Let ϕ_3 be the FFCF. There is ample evidence that this correlation function relaxes more slowly in the proximity of the isotropic−nematic transition, but it is also reasonable to suspect that it can be influenced by large wave vector density fluctuations. This suggests a schematic MCT equation of the form

$$\ddot{\phi}_3(t) + \mu_3\dot{\phi}_3(t) + \Omega_3^2\phi_3(t) + \Omega_3^2\int_0^t d\tau m_3(t-\tau)\dot{\phi}_3(\tau) = 0 \tag{10}$$

Ω_3 is a molecular oscillator frequency, and μ_3 is a damping constant. The memory function in this equation is

$$m_3(t) = \lambda\phi_1(t)\phi_3(t) + \beta\phi_2(t)\phi_3(t) \tag{11}$$

where λ and β are the coupling constants that describe the effect, on the decay of ϕ_3, of ϕ_1 and ϕ_2, respectively. The initial conditions are $\phi_3(0) = 1$ and $\dot{\phi}_3(0) = 0$.

Equations 8−11 are a schematic mode coupling model for three correlators. The model was constructed by making standard schematic MCT assumptions. In addition, the physics of Landau−de Gennes theory has been incorporated into the equation of motion for ϕ_2, the collective orientation correlation function. Finally, the equation of motion of ϕ_3 contains a coupling to ϕ_2 as well as to ϕ_1 to take into account the effect of the isotropic−nematic transition on the long time dynamics of the FFCF, ϕ_3.

Although schematic MCT can suggest forms for the kinetic equations of slowly relaxing correlation functions, it provides no way of calculating the values of the parameters that appear in the equations. These parameters are in general temperature dependent. Thus, a schematic MCT model alone cannot be used to make predictions about observable correlation functions.

However, if experimental data about the time dependence of a slowly relaxing correlation function is available, it is in general

DOI: 10.1021/acs.jpcb.6b04997
J. Phys. Chem. B 2016, 120, 7003−7015

possible to use schematic models in the following way. First, numerical methods are prepared that enable the computation of the correlation functions for any set of parameters. Then, for each temperature of each system studied, the parameters are allowed to vary to generate the correlation functions that best fit the experimental data. If that best fit is inadequate, then it is clear that the schematic model is not applicable. If the best fit is adequate, this suggests (but does not prove) that the assumptions made in constructing the model are correct.

This procedure has been used by Götze and co-workers and others to analyze experimental data of many different types of relaxation processes.[19,20,30,43−45] The extension of this procedure to nematogens has been applied to analyze OHD-OKE data on liquid crystals in the isotropic phase.[17] In many of these cases, the correlation experimental functions are fit in a convincing way.

If we have both OHD-OKE and 2D IR data on the same system, the OHD-OKE correlation function is the time derivative of ϕ_2, and the OHD-OKE data can be used to determine the best values of the constants in eqs 8 and 9. This was the procedure of Li et al.[19] The 2D IR FFCF data are ϕ_3, and the data can be used to determine the best values of the constants in eqs 10 and 11. Results of this analysis for several systems will be discussed below.

IV. RESULTS AND DISCUSSION

IV.A. OHD-OKE Results for Three Liquid Crystals Approaching T_{NI}.

IV.A.1. Data for the Three Liquid Crystals. We have previously studied the OKE decay of 5CB (both neat and doped with small amounts of 5SeCB), 8CB, and 5PCH at a variety of temperatures in the isotropic phase.[10−12,23,34] In all cases, the data could be fit with eq 4. The two power law exponents for all systems were found to be independent of temperature. Power law exponents are not identical across liquid crystal systems, but power law exponents were found to be unchanged within experimental error when a small amount of 5SeCB was added to neat 5CB.[24] In all cases, the final exponential is the Landau−de Gennes decay constant (τ_{LdG}); a plot of viscosity, η, over τ_{LdG} versus temperature produced a straight line with x-intercept equal to T^*. The addition of a small amount of 5SeCB lowered T^* by ∼3 K but did not perturb the liquid crystal nature of 5CB.

OHD-OKE decays of 2.5 mol % 5SeCB in both 8CB and 5PCH were collected at a range of temperatures above the isotropic−nematic phase transition; Figure 1 shows three temperatures for both the doped 8CB (A) and 5PCH (B) samples. (The middle curve in panel B also has a red dashed fit line from the schematic MCT description of the isotropic phase orientational dynamics, discussed below.) Each of the decays can be fit with the phenomenological eq 4. As in the case for neat liquids, the power law exponents are found to be independent of temperature. The intermediate power law has exponent z = 0.56 and 0.74 for 5SeCB doped 8CB and 5PCH, respectively. The von Schweidler power law has an exponent b − 1 = −0.03 and −0.04 again for 5SeCB doped 8CB and 5PCH, respectively. For both liquids, these exponents agree with those found for the corresponding neat liquids reported previously.[13,34] The agreement suggests that the addition of 5SeCB has little effect on the caging dynamics for either of the liquid crystals, which was also true for the previous studies of 5CB.

Fitting the data according to eq 4 more importantly permits the determination of τ_{LdG}. With the addition of viscosity data,

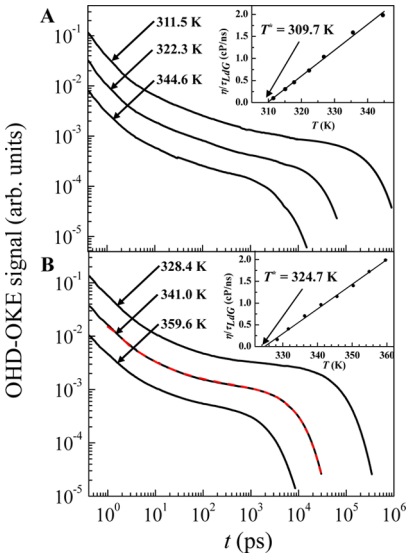

Figure 1. Temperature-dependent OHD-OKE data for 2.5 mol % 5SeCB in 8CB (A) and 5PCH (B). The curves have been offset along the vertical axis for clarity. Each decay was fit with the function given by eq 4. The insets show Landau−de Gennes plots from the results for the long time exponential decay and viscosity data. The x-intercept of the linear fit gives T^* = 309.7 K and T^* = 324.7 K for doped 8CB and 5PCH, respectively. The red dashed curve is a representative fit to the data of the time derivative of ϕ_2 obtained from a joint solution to the schematic MCT eqs 7 and 8.

Landau−de Gennes plots for the doped liquid crystal samples can be constructed (Figure 1 insets).[46,47] It is clear that both 8CB and 5PCH doped with 5SeCB obey Landau−de Gennes theory, as η/τ_{LdG} versus temperature is linear. The x-intercepts of these lines are found to be 309.7 ± 0.5 and 324.7 ± 0.5 K for 5SeCB doped 8CB and 5PCH, respectively. Neat 8CB is reported to have T^* = 313 K; neat 5PCH is reported to have T^* = 328 K.[13,17] As was previously observed, the addition of a small amount of vibrational probe lowers the phase transition temperature of the liquid crystals by a few degrees.[23,24] More importantly, the liquid crystal natures of 8CB and 5PCH are maintained upon the addition of 5SeCB. 5SeCB is similar in size and shape to all three nematogens that were studied. The relatively small change in transition temperature and the strict adherence to the Landau−de Gennes temperature dependence allows us to confidently use 5SeCB as a vibrational probe without significantly perturbing the dynamics within the pseudonematic domains.

IV.A.2. Interpretation of the Data Using the MCT Schematic Model. The OHD-OKE data can be analyzed and interpreted using the schematic MCT model in eqs 8 and 9 using the method discussed in section III. Li et al. reported such an analysis for neat 5CB and 5PCH, and we have previously analyzed the 5SeCB doped 5CB data in the same manner.[17] In accordance with previous studies, the molecular oscillator frequencies were held constant at Ω_1 = 0.5 THz and Ω_2 = 1 THz.[20,23,30] The Landau−de Gennes constant Γ was set equal to τ_{LdG}^{-1} as obtained from the fits to eq 4. The OHD-OKE data were initially fit at all temperatures with the remaining parameters allowed to vary with temperature. The values of μ_1, ν_1, and ν_2 were found to be virtually independent of temperature. Final fits of all data (see red dashed curve on the middle data set of Figure 1B) were performed with these parameters held constant at their average value. It is worth

DOI: 10.1021/acs.jpcb.6b04997
J. Phys. Chem. B 2016, 120, 7003−7015

noting that all of the parameters in the density correlation function, ϕ_1, are found to be essentially independent of temperature, and all of the temperature dependence appears in the orientational correlation function.

As was previously observed for neat liquid crystals, the values of the remaining free parameters, μ_2 and κ, for the doped systems studied here were found to increase rapidly as the nematic−isotropic phase transition was approached from above.[17] Plots of $1/\mu_2$ and $1/\kappa$ for 2.5 mol % 5SeCB in 8CB and 5PCH are shown in Figure 2. Also included on these plots

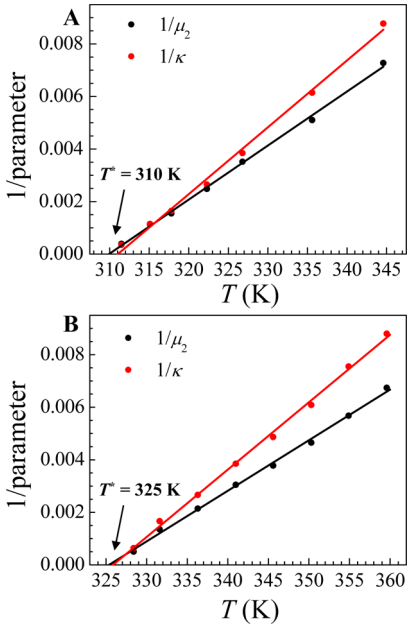

Figure 2. Temperature dependence of μ_2 and κ for 2.5 mol % 5SeCB in 8CB (A) and 5PCH (B). MCT curves for doped 8CB were calculated for Ω_1 = 0.5 THz, Ω_2 = 1 THz, μ_1 = 1.29 THz, ν_1 = 0.99 and ν_2 = 0.26. MCT curves for doped 5PCH were calculated for Ω_1 = 0.5 THz, Ω_2 = 1 THz, μ_1 = 1.35 THz, ν_1 = 0.99 and ν_2 = 0.51. Within experimental error, both μ_2 and κ diverge at T^*.

are linear fits to the data, extrapolated to intersect the x-axis. Within experimental error, the x-intercept for all lines matches the T^* value for the corresponding doped liquid crystal found from the Landau−de Gennes plots. The same behavior was previously found for 5CB.

IV.B. 2D IR Results for Three Liquid Crystals Approaching T_{NI}. *IV.B.1. Data for the Three Liquid Crystals.* We have previously reported spectral diffusion measurements of 2.5 mol % 5SeCB in 5CB at 11 temperatures above T_{NI}.[24] At all temperatures, the CLS(T_w) could be fit to a triexponential decay. The time constants for spectral diffusion were found to be remarkably comparable to a structurally similar non-mesogenic liquid when at least 5 K above T_{NI}. However, the decay constants for spectral diffusion diverged as T_{NI} is approached from above. The temperature dependence of the middle and long time constant can be fit to the form $t = A|T - x_c|^p$. Within experimental error, we found that $x_c = T^*$ and $p = -1/2$ for both t_{mid} and t_{long} (see Table 1). Greater uncertainty exists in the shortest decay constant, as the nonresonant signal from the sample is quite large, and therefore, the data quality of the fast component was not sufficient to fit. Note that the divergence in the time constants for spectral diffusion matches the temperature dependence given for the size of the

Table 1. Temperature Dependence of Spectral Diffusion Time Constants

liquid crystal		A	x_c	$-p$
5CB	t_{mid}	85 ± 18	305.6 ± 0.5 K	0.52 ± 0.06
	t_{long}	502 ± 32	306.7 ± 0.1 K	0.48 ± 0.03
8CB	t_{mid}	56 ± 18	310.5 ± 1.0 K	0.43 ± 0.10
	t_{long}	530 ± 80	310.2 ± 0.7 K	0.44 ± 0.06
5PCH	t_{mid}	80 ± 15	324.5 ± 0.8 K	0.51 ± 0.06
	t_{long}	628 ± 72	325.9 ± 0.2 K	0.52 ± 0.04
global	t_{long}	28 ± 9	−0.0003 ± 0.0003	0.54 ± 0.06

pseudonematic domains, eq 1, and not the time for total orientational relaxation, eq 2. Additionally, the total orientational relaxation is orders of magnitude slower than the time scale for spectral diffusion. Thus, complete orientational randomization is not required for the vibrational probe to experience all structural environments that contribute to the inhomogeneous line shape.

We have collected 2D IR data for the liquid crystals 8CB and 5PCH at temperatures approaching their respective T_{NI} for comparison with the results for 5CB. We showed with OHD-OKE experiments in the previous section that the addition of a long-lived vibrational probe does not disturb the liquid crystal dynamics. The CN stretch transition of 5SeCB occurs at 2155 cm^{-1} with a FWHM of ∼9.5 cm^{-1} in both liquid crystals. The vibrational lifetimes of 5SeCB in 8CB and 5PCH were found to be 320 ± 5 and 340 ± 6 ps independent of temperature. The long lifetime permits the collection of 2D IR data to ∼1 ns.

8CB is a member of the *n*CB family; unlike 5CB, 8CB possesses a smectic A phase at temperatures below the nematic phase before crystallization. 2D IR experiments were conducted on 2.5 mol % 5SeCB in 8CB at 14 temperatures in the isotropic phase. Data at six temperatures (311.3, 311.6, 312.0, 312.4, 313.2, and 313.3 K) were taken within 5° of T_{NI}. It was at temperatures close to T_{NI} in 5CB where divergent behavior was previously observed; it is in this region that the size of the pseudonematic domains is changing dramatically. Representative 8CB CLS(T_w) decays at four temperatures are shown in Figure 3A. Data at these and all other temperatures can be fit with a triexponential decay. The resulting FFCF parameters for all of the fits can be found in Table 2.

As previously observed for 5CB, the time scale for spectral diffusion slows gradually as the temperature is lowered from 350 K to approximately 5 K from the phase transition. However, as the temperature is lowered even by tenths of a degree near T_{NI}, the CLS(T_w) decay constants slow dramatically. There is significant uncertainty in the shortest time constant due to the large nonresonant signal in the sample. A plot of the longest decay constant (t_{long}) versus temperature is shown in Figure 3B. The temperature dependence of the middle and long time constant can be fit to the form $t = A|T - x_c|^p$, just as was previously found for 5CB. The resulting fit for the longest time constant is shown in Figure 3B, and fit parameters are in Table 1. Within experimental error, $x_c = T^*$ found from OHD-OKE experiments, for both the middle and longest time constants. The divergence at T^* is characterized by the fitted exponent $p = -1/2$. The temperature dependence of the long time constant can be recast to match eq 1 for $\xi(T)$, yielding

$$t_{long} = a_{long}\left(\frac{T^*}{T - T^*}\right)^{1/2} \quad (12)$$

DOI: 10.1021/acs.jpcb.6b04997
J. Phys. Chem. B 2016, 120, 7003−7015

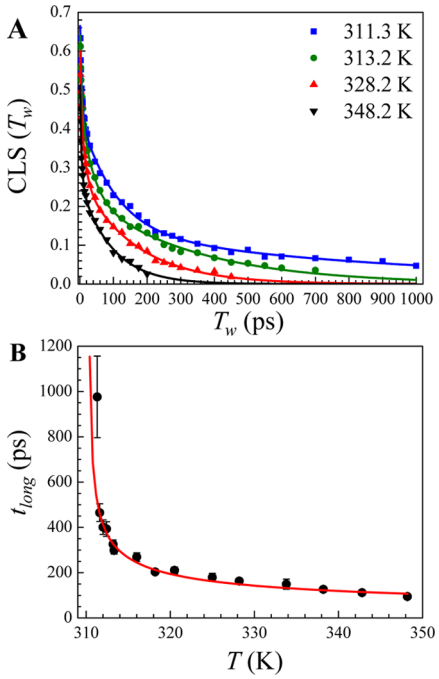

Figure 3. (A) 2D IR CLS(T_w) data for 2.5 mol % 5SeCB in 8CB at four temperatures with triexponential decay fits. The resulting FFCF parameters at all temperatures are given in Table 2. (B) Longest decay constant from the triexponential decay as a function of temperature. The time constants are fit to the form $A|T\text{-}x_c|^p$, shown in red.

where a_{long} is a scaling factor equal to 30 ± 5 ps. a_{long} for 5CB was previously found to be 29 ± 2 ps.[24] Not only is the same divergence for the time scale of spectral diffusion observed for 8CB as 5CB, but the scaling factors are identical. The agreement in functional form and scaling between 5CB and 8CB is suggestive of a universal property of nematic liquid crystals in the isotropic phase but requires examination of a nematic liquid crystal outside of the *n*CB family.

The substituted phenylcyclohexanes (PCHs) were developed by Eidenschink et al. in 1977 as a new class of chemically stable, low melting, and colorless nematic liquid crystals.[48] Compared to analogous biphenyls, the substituted PCHs have a weaker polarizability anisotropy.[49] The resulting lower optical anisotropy of PCH enabled the construction of twisted nematic liquid crystal displays with a smaller angle dependence on the contrast ratio. Relative to 5CB and 8CB, 5PCH has chirality and a lower viscosity.[46,47,49]

2D IR experiments were conducted on 2.5 mol % 5SeCB in 5PCH at 10 temperatures in the isotropic phase. Data at four temperatures (326.5, 326.8, 327.1, and 327.6 K) were taken within 2° of T_{NI}. Representative CLS(T_w) decays at three temperatures are shown in Figure 4A.

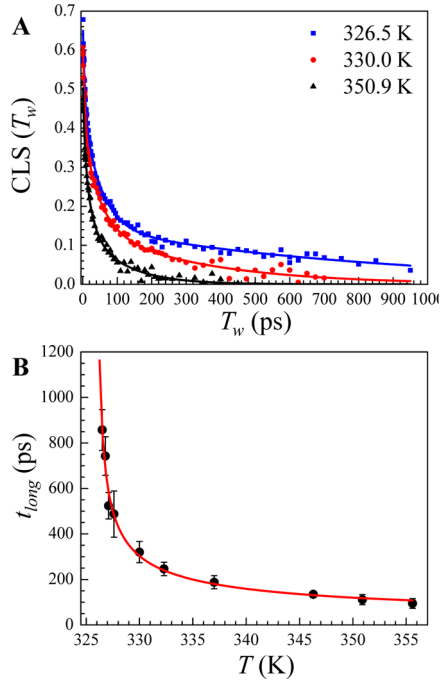

Figure 4. (A) 2D IR CLS(T_w) data for 2.5 mol % 5SeCB in 5PCH at three temperatures with triexponential decay fits. The resulting FFCF parameters at all temperatures are give in Table . (B) Longest decay constant from the triexponential decay as a function of temperature. The time constant is fit to the form $A|T\text{-}x_c|^p$, shown in red.

Data in Figure 4A and all other temperatures can be fit with a triexponential decay. The resulting FFCF parameters for all of the fits can be found in Table 3. As observed for 5CB and 8CB, spectral diffusion time constants slow gradually when the temperature is lowered far from the phase transition. When the

Table 2. FFCF Parameters for 2.5 mol % 5SeCB in 8CB

T (K)	T_2 (ps)	Γ (cm^{-1})	Δ_1 (cm^{-1})	t_1 (ps)	Δ_2 (cm^{-1})	t_2 (ps)	Δ_3 (cm^{-1})	t_3 (ps)
311.3	4.2 ± 0.4	2.5 ± 0.3	1.7 ± 0.2	5.3 ± 0.5	2.0 ± 0.2	104 ± 9	1.3 ± 0.2	976 ± 180
311.6	4.9 ± 0.4	2.1 ± 0.2	1.8 ± 0.2	4.2 ± 0.5	1.8 ± 0.2	54 ± 7	1.8 ± 0.2	465 ± 39
312.0	4.7 ± 0.5	2.3 ± 0.2	1.7 ± 0.2	3.4 ± 0.5	1.8 ± 0.2	45 ± 7	1.8 ± 0.2	401 ± 32
312.4	4.2 ± 0.4	2.5 ± 0.3	1.7 ± 0.2	3.8 ± 0.4	1.7 ± 0.2	57 ± 7	1.7 ± 0.2	393 ± 32
313.2	4.2 ± 0.4	2.5 ± 0.3	1.5 ± 0.2	4.2 ± 0.7	1.8 ± 0.2	35 ± 5	1.8 ± 0.2	325 ± 20
313.3	4.9 ± 0.5	2.2 ± 0.2	1.6 ± 0.2	2.7 ± 0.8	1.8 ± 0.2	34 ± 4	1.9 ± 0.2	298 ± 16
316.0	4.7 ± 0.5	2.3 ± 0.2	1.7 ± 0.2	2.4 ± 1	1.8 ± 0.2	30 ± 5	1.9 ± 0.2	269 ± 19
318.2	4.4 ± 0.4	2.4 ± 0.2	1.7 ± 0.2	2.4 ± 0.5	1.4 ± 0.2	22 ± 4	2.0 ± 0.2	203 ± 7
320.5	3.8 ± 0.4	2.8 ± 0.3	1.4 ± 0.2	3.7 ± 3.2	1.5 ± 0.2	24 ± 9	2.0 ± 0.2	210 ± 15
325.0	5.1 ± 0.5	3.1 ± 0.3	2.0 ± 0.2	2.3 ± 0.6	1.8 ± 0.2	29 ± 5	1.7 ± 0.2	179 ± 18
328.2	3.9 ± 0.4	2.7 ± 0.3	1.3 ± 0.2	1.9 ± 0.7	1.7 ± 0.2	14 ± 2	1.9 ± 0.2	163 ± 6
333.8	3.8 ± 0.4	2.8 ± 0.3	1.9 ± 0.2	3 ± 1.1	1.7 ± 0.2	32 ± 9	1.5 ± 0.2	149 ± 22
338.2	4.1 ± 0.4	2.6 ± 0.3	1.5 ± 0.2	1.8 ± 0.8	1.6 ± 0.2	13 ± 2	1.8 ± 0.2	126 ± 5
342.8	3.7 ± 0.4	2.8 ± 0.3	2.0 ± 0.2	2.9 ± 1.4	1.8 ± 0.2	19 ± 4	1.5 ± 0.2	112 ± 11
348.2	3.8 ± 0.4	2.8 ± 0.3	1.6 ± 0.2	3 ± 4	1.4 ± 0.2	6 ± 8	1.8 ± 0.2	94 ± 5

DOI: 10.1021/acs.jpcb.6b04997
J. Phys. Chem. B 2016, 120, 7003−7015

Table 3. FFCF Parameters for 2.5 mol % 5SeCB in 5PCH

T (K)	T_2 (ps)	Γ (cm^{-1})	Δ_1 (cm^{-1})	t_1 (ps)	Δ_2 (cm^{-1})	t_2 (ps)	Δ_3 (cm^{-1})	t_3 (ps)
326.5	3.7 ± 0.4	2.8 ± 0.3	2.0 ± 0.2	8.0 ± 0.9	2.3 ± 0.2	60 ± 6	1.5 ± 0.2	857 ± 90
326.8	4.0 ± 0.4	2.7 ± 0.3	2.2 ± 0.2	5.5 ± 0.6	2.3 ± 0.2	57 ± 5	1.4 ± 0.2	742 ± 85
327.1	3.6 ± 0.4	2.9 ± 0.3	2.1 ± 0.2	6.1 ± 0.7	2.2 ± 0.2	48 ± 5	1.5 ± 0.2	524 ± 58
327.6	3.3 ± 0.3	3.3 ± 0.3	2.0 ± 0.2	7.5 ± 0.9	2.1 ± 0.2	65 ± 10	1.4 ± 0.2	487 ± 101
330.0	3.5 ± 0.3	3.1 ± 0.3	2.0 ± 0.2	6.8 ± 1.1	2.1 ± 0.2	48 ± 9	1.6 ± 0.2	320 ± 47
332.3	3.0 ± 0.3	3.5 ± 0.3	1.6 ± 0.2	5.4 ± 1.2	2.0 ± 0.2	28 ± 6	1.9 ± 0.2	246 ± 29
337.0	2.8 ± 0.3	3.8 ± 0.4	1.8 ± 0.2	4.1 ± 1.0	2.0 ± 0.2	28 ± 6	1.5 ± 0.2	188 ± 29
346.3	2.9 ± 0.3	3.7 ± 0.4	1.9 ± 0.2	0.9 ± 0.3	2.0 ± 0.2	18 ± 1.5	1.5 ± 0.2	134 ± 13
350.9	2.7 ± 0.3	3.9 ± 0.4	1.6 ± 0.2	5.1 ± 2.2	2.0 ± 0.2	22 ± 9	1.6 ± 0.2	111 ± 22
355.6	3.3 ± 0.3	3.3 ± 0.3	1.7 ± 0.2	2.5 ± 1.0	2.4 ± 0.2	18 ± 4	1.5 ± 0.2	94 ± 21

temperature is lowered close to T_{NI}, the CLS(T_w) decay constants slow much more dramatically. A plot of the longest decay constant (t_{long}) versus temperature is shown in Figure 4B. The temperature dependence of the middle and longest time constant can be fit to the form, $A|T - x_c|^p$; the resulting parameters are in Table 1. Within experimental error, $x_c = T^*$ and $p = -1/2$ for both the middle and long time constants. Rewriting the fit of the long time constant to match eq 12, we find that a_{long} for 5PCH is 34 ± 4 ps.

To demonstrate the universal behavior of the three liquid crystal systems, the temperature dependence of t_{long} can be rescaled. Figure 5 transforms the x-axis to $(T - T^*)/T^*$, where

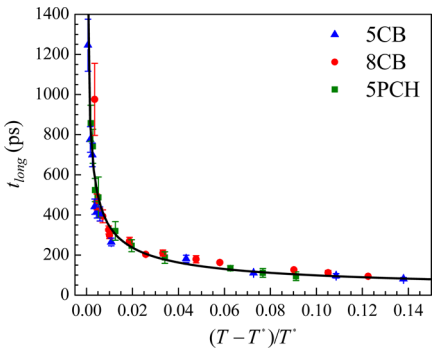

Figure 5. Slowest spectral diffusion time constant as a function of reduced temperature for three liquid crystals in the isotropic phase. The black curve is a fit of the data to the equation $A\left|\left(\frac{T-T^*}{T^*}\right) - x_c\right|^p$. Fit parameters are given in Table 1.

T^* values are taken from OHD-OKE measurements of the doped liquid crystals. Data points for all three liquid crystals fall on the same curve, and a combined fit to $t_{long} = A\left|\left(\frac{T-T^*}{T^*}\right) - x_c\right|^p$ is shown as the solid black line in Figure 5. Again, we find that $p = -1/2$ and the divergence occurs at $T = T^*$ (Table 1). Not only does temperature dependence of spectral diffusion have the same form in all liquid crystals studied, but a simple linear rescaling of the temperature produces a single curve. Universality of several properties in the nematic phase upon rescaling of the temperature axis has previously been shown, but this has also required a normalization at a common rescaled temperature.[50] Here, no such normalization was required. It is possible that a normalization might result in slightly more convergence, but any such scaling must be minor. For instance, a scaling based on viscosity can be ruled out, as 5PCH is roughly half as viscous as 5CB at the same reduced temperature, which is in turn less viscous than 8CB.[46,49]

IV.B.2. Interpretation of the Data Using the MCT Schematic Model. The 2D IR data for the three nematogens, at 10 or more temperatures for each nematogen, were analyzed and interpreted using the schematic MCT model in eqs 8−11 using the method discussed in section III. The first step is to use the OHD-OKE data for the same material at the same temperature to obtain values of the parameters in eqs 8 and 9 as discussed above. For the three liquid crystals studied here, ϕ_1 was found to be temperature independent over the experimental range of temperatures. Therefore, precisely matching the temperature of the OHD-OKE data to the 2D IR data was not a factor for obtaining the ϕ_1 parameters. If OHD-OKE data were not collected at a temperature matching a given 2D IR CLS(T_w) decay, ϕ_2 was simulated using parameters μ_2, κ, and Γ obtained from the linear fits of their temperature dependences (see Figure 2 and the insets in Figure 1). Slight variations in μ_2, κ, and Γ were tested, and essentially no change was observed in the calculated ϕ_3 curve.

As has been previously suggested for Ω_1 and Ω_2, we choose a value for Ω_3 in the terahertz regime. If Ω_3 is held at too small a value, oscillations develop in the early time ϕ_3 curve. Large values of Ω_3 are not physical, as the molecular oscillator frequency would be well above the bath modes of the liquid. Within these constraints, variation in Ω_3 leads to corresponding changes in μ_3 but no change in the quality of fits. Thus, we have chosen Ω_3 = 1 THz for all temperatures and all three liquids.

We first consider 5CB. In initial fits of the 2D IR data, μ_3, λ, β, and a scaling factor were all allowed to vary under the constraint that all values were positive. We found that μ_3 was essentially independent of temperature. Holding μ_3 constant at the average value did not significantly change the quality of the fits or trends observed in λ and β. In the final fits, μ_3 was set equal to 10 THz at all temperatures. The temperature dependence of λ and β will be presented and discussed later in the section.

Figure 6 shows CLS(T_w) decays for 5CB at temperatures near the phase transition (307.5 K) and well above the phase transition (349 K). The blue curves are triexponential fits to the data; the red curves are fits using the ϕ_3 model given by eqs 10 and 11. The quality of fits to CLS(T_w) data at other temperatures is similar. In fitting with the multiexponential function, exponentials were added until the fit could not be improved. A triexponential fit to the data requires six free parameters: three decay constants and three amplitude factors. The MCT model requires only three parameters to essentially produce an identical fit. The residuals of the triexponential fit and the ϕ_3 model of the CLS(T_w) data at 307.5 K are shown in

DOI: 10.1021/acs.jpcb.6b04997
J. Phys. Chem. B 2016, 120, 7003−7015

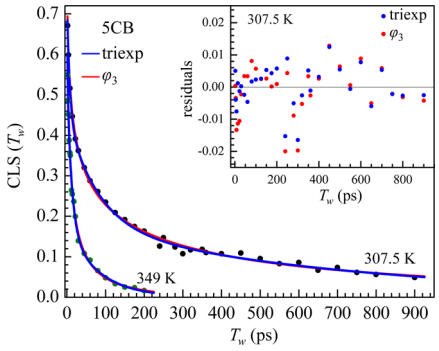

Figure 6. CLS(T_w) data for 2.5 mol % 5SeCB in 5CB at 307.5 K (green points) and 349 K (black points). The data are fit with a triexponential decay (blue) and with ϕ_3 (red) as defined in eqs 9 and 10. The inset shows the residuals of the triexponential function (six temperature dependent parameters) and ϕ_3 (three temperature dependent parameters) fits for the 307.5 K CLS(T_w) data.

the inset. The error in fitting with either method falls within error of the CLS(T_w) data points themselves, and no systematic error with the MCT model is observed. The quality of the fit to the 2D IR data with the MCT calculation of ϕ_3 is as good as the triexponential function, with half the number of temperature dependent parameters.

To further test the MCT model, we used the same type of analysis for the two additional nematogens, 8CB and 5PCH. The fitting procedure is identical to that described for 5CB. Ω_3 was fixed at 1 THz, and once again, μ_3 was found to be insensitive to temperature. For both liquid crystals, we held μ_3 = 10 THz, and all data were fit. Figure 7A shows CLS(T_w) decays for 8CB at a temperature near (311.6 K) and significantly removed (338.2 K) from T_{NI}. Figure 7B shows similar data for 5PCH at 326.5 and 355.6 K. Triexponential fits to the data are shown as blue curves; fits using the MCT model are in red. The quality of the fits to the CLS(T_w) data at other temperatures is similar. As was the case for 5CB, fits with a triexponential decay or MCT are nearly identical. For all temperatures of the three liquid crystals, 5CB, 8CB, and 5PCH, only three temperature dependent parameters and two temperature independent parameters are needed to fit the 2D IR data with the MCT theory at the temperatures studied.

It is important to emphasize that the ϕ_1 and ϕ_2 inputs for the calculation of ϕ_3 come from an entirely separate set of temperature dependent measurements using the OHD-OKE experiments. The OHD-OKE experiments measure the orientational relaxation dynamics of the liquid. Fitting the OHD-OKE data over many decades of time using the liquid crystal version of the schematic MCT yields the large wave vector density correlation function, ϕ_1, and the orientation correlation function, ϕ_2. Once ϕ_1 and ϕ_2 are determined at each temperature, the parameters that define them are fixed in the fits to the 2D IR CLS(T_w) decay using ϕ_3.

The two most important temperature dependent parameters are λ and β, which determine the strength of the effect that ϕ_1 and ϕ_2, respectively, have on ϕ_3. Plots of λ and β as a function of temperature for 5CB are shown in Figure 8. The λ and β coupling parameters are not monotonic functions of temperature. They change behavior ~5 K above T_{NI}, the temperature at which the spectral diffusion dynamics begin to display the divergent slowing.

As the temperature is lowered, the coupling to ϕ_1 initially increases while the coupling to ϕ_2 decreases. When the

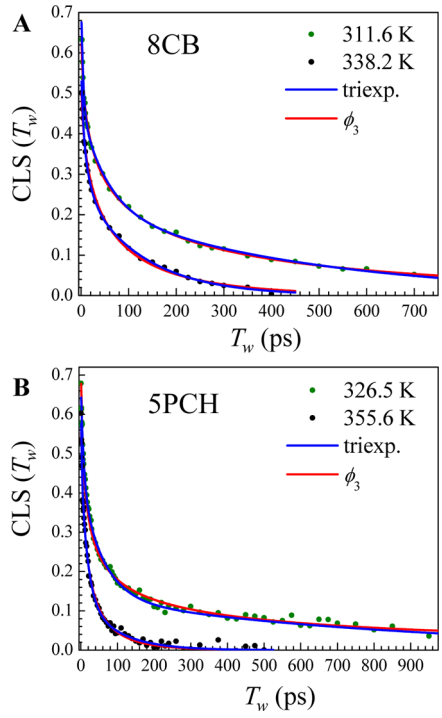

Figure 7. (A) CLS(T_w) data for 2.5 mol % 5SeCB in 8CB at 311.6 K (green) and 338.2 K (black). The data are fit with a triexponential decay (blue) and with ϕ_3 (red) as defined in eqs 9 and 10. ϕ_1 and ϕ_2 are calculated from OHD-OKE experiments; Ω_3 = 1 THz and μ_3 = 10 THz. (B) CLS(T_w) data for 2.5 mol % 5SeCB in 5PCH at 326.5 K (green) and 355.6 K (black). The data are fit with a triexponential decay (blue) and with ϕ_3 (red) as defined in eqs 9 and 10. ϕ_1 and ϕ_2 are calculated from OHD-OKE experiments; Ω_3 = 1 THz and μ_3 = 10 THz.

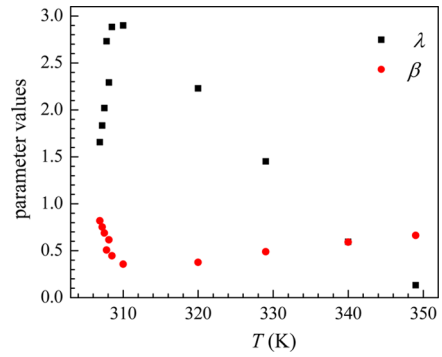

Figure 8. Temperature dependence of the coupling parameters λ (black) and β (red) found in the memory function for ϕ_3 for the liquid crystal 5CB. Both coupling constants show a dramatic change in behavior at ~310 K, where the slowing of spectral diffusion in 5CB relative to 5B is first noticeable.

temperature reaches 310 K (roughly 5 K above T^*), the behaviors of the coupling parameters λ and β reverse. Suddenly, the FFCF correlator ϕ_3 begins to lose coupling to ϕ_1, the large wave vector density correlator, and picks up coupling to ϕ_2, the orientational correlation function. At these temperatures, ϕ_1 is identical to its value at high temperatures while ϕ_2 is slowing down dramatically due to the growing size of pseudonematic domains. It is at 310 K where evidence of critical slowing in the spectral diffusion of 5CB is first noticed compared to the nonmesogenic 5B.[23,24] An increase in coupling to the slowing

DOI: 10.1021/acs.jpcb.6b04997
J. Phys. Chem. B 2016, 120, 7003−7015

ϕ_2 allows ϕ_3 to pick up the critical slowing due to the approach to T_{NI} that is built into ϕ_2 through the Γ parameter.

The temperature dependences of the coupling constants for 8CB and 5PCH show similar trends, Figure 9, as a function of

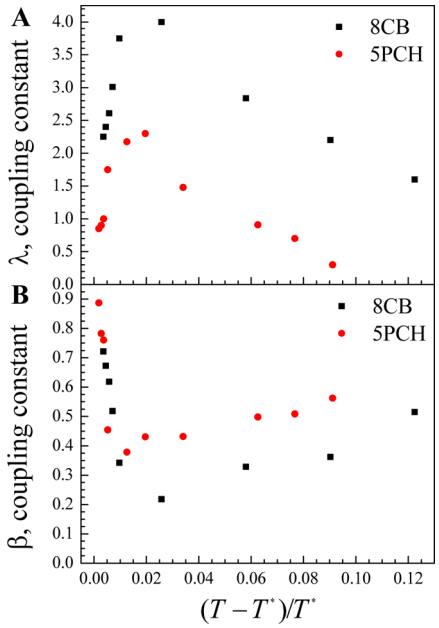

Figure 9. Reduced temperature dependence of the coupling parameters λ (A) and β (B) found in the memory function for ϕ_3 for the liquid crystal 8CB (black) and 5PCH (red). The coupling constants show the same trends as in 5CB.

reduced temperature. For both liquid crystals, λ gradually increases as the temperature is lowered and then drops sharply. The coupling constant β shows the opposite behavior, decreasing slightly with decreasing temperature and then rising sharply. This behavior is the same as found for 5CB, as shown in Figure 8. The turning point for these coupling constants in both liquid crystals again occurs in the neighborhood of $(T - T^*)/T^* = 0.02$, near 5 K above T_{NI}. Analysis using the MCT model applied to the temperature dependent dynamics measured with the 2D IR experiments indicates that the dramatic growth of pseudonematic domains within a few degrees of the phase transition temperature produces a remarkable change in the coupling to the types of motions that produce frequency fluctuations.

We propose that the temperature dependence of the experimentally observed FFCF, which is modeled by ϕ_3, is the result of a small wave vector (long wavelength) density correlation function, which is critically slowing as the isotropic−nematic phase transition is approached from above. Both density and orientational fluctuations could conceivably contribute to the loss of frequency correlation of a vibrational probe. As shown below, experimental evidence excludes both collective orientational relaxation and probe orientational relaxation as possible sources of spectral diffusion.[23]

Collective orientational relaxation for the isotropic phase liquid crystals measured with OHD-OKE experiments is orders of magnitude slower than the FFCF decay at all temperatures.[23] MCT calculations using eqs 8 and 9 generate the orientational correlation function, and then, the derivative is taken to compare with the OHD-OKE data. Over the experimental time scale of the FFCF decay to zero, the orientational correlation function decays only a few percent. Thus, orientational randomization of the pseudonematic domains is much too slow to be the source of complete spectral diffusion measured with 2D IR.

We have previously performed polarization selective pump−probe experiments on both 5SCB and 5SeCB in 5CB at several temperatures in the isotropic phase.[23,24] By collecting pump−probe signals at multiple polarizations, it was possible to extract information on both the vibrational lifetime and the orientational relaxation of the probe. At all temperatures, the orientational relaxation of the probe molecule was found to be negligible over the time scale of spectral diffusion. Thus, the pseudonematic domains' orientation correlation and the reorientation of an individual molecule (the vibrational probe) within the domains are virtually static on the time scale of the decay of the FFCF. Thus, orientational fluctuations cannot be contributing to the spectral diffusion or the inhomogeneous line shape of the probe.

Once orientational fluctuations have been ruled out as a source of spectral diffusion, we turn to density fluctuations. The F_{12} model for ϕ_1 presented in eqs 8a and 9a is an approximation for the large wave vector density fluctuations. Unlike the orientational relaxation, ϕ_1 decays roughly 90% in a few hundred picoseconds. This is approximately the time scale of the spectral diffusion. However, the functional form of the ϕ_1 decay is vastly different from that of the 2D IR CLS(T_w) decays. Furthermore, the temperature dependence of ϕ_1 does not match that of the FFCF decay. Over the range of temperatures studied, all well above any freezing temperature, ϕ_1 is temperature independent in the fits to the OHD-OKE data. For supercooled liquids, ϕ_1 is the large wave vector density correlation function which critically slows approaching the MCT transition temperature from above. Modifications to schematic MCT to account for the isotropic−nematic transition yield only an approximation of the time dependence of the large wave vector density fluctuations, but it is clearly observed that ϕ_1 is not showing the critical slowing approaching T_{NI} that is seen in the spectral diffusion for three liquid crystals.

Excluding orientational fluctuations and very local (large wave vector) density fluctuations as the source of spectral diffusion leaves small wave vector (long wavelength) density fluctuations as the cause of spectral diffusion in isotropic liquid crystals. Long range density fluctuations have previously been proposed as a source of inhomogeneous broadening in the vibrational absorption line shapes.[51] The divergence of the rate constants for spectral diffusion can then be considered as a critical slowing of small wave vector density fluctuations related to a growing density correlation length as the isotropic−nematic phase transition is approached from above.

V. CONCLUDING REMARKS

Ultrafast infrared spectroscopy and optical heterodyne detected-optical Kerr effect experiments were used in tandem to study the structural dynamics in the isotropic phase of three liquid crystals, 5CB, 8CB, and 5PCH. A small amount of 5SeCB was added to each of the liquid crystals to serve as a long-lived vibrational probe for infrared experiments. We confirmed that the addition of 5SeCB did not disturb the liquid crystal properties, other than lowering T_{NI} by a few degrees.

The orientational relaxation of liquid crystals in the isotropic phase is dominated by the complete randomization of

DOI: 10.1021/acs.jpcb.6b04997
J. Phys. Chem. B 2016, 120, 7003−7015

pseudonematic domains characterized by a correlation length ξ. The size of the pseudonematic domains grows as $[T^*/(T - T^*)]^{1/2}$ as the phase transition temperature is approached from above. Previous results on 5CB showed that the time constants for spectral diffusion slow with the same temperature dependence as ξ. 2D IR experiments on 5SeCB in 8CB and 5PCH at many temperatures above T_{NI} presented here show that the decay constants for spectral diffusion for both liquids have precisely the same temperature dependence. When the temperature is rescaled as the reduced temperature $(T - T^*)/T^*$, the longest time constants for spectral diffusion for all three liquids are found to fall on a common curve (see Figure 5 and Table 1). The results for the three liquid crystals are suggestive of universal pretransitional phenomena for the nematic–isotropic phase.

To further understand the source of critical slowing of the spectral diffusion, we have developed an MCT model for the FFCF, ϕ_3, given in eqs 10 and 11. The model for ϕ_3 constructed here has roots in schematic MCT for an experimental observable coupled to the correlator that undergoes the mode coupling transition. ϕ_3 couples to both the large wave vector density (ϕ_1) and orientational (ϕ_2) correlators obtained from OHD-OKE experiments. Coupling to ϕ_2 allows ϕ_3 to account for frequency fluctuations that are not due solely to the approach to the mode coupling temperature, but instead approach to the nematic–isotropic phase transition. We have found that ϕ_3 can accurately reproduce the 2D IR data with only three temperature dependent parameters at all temperatures, for all three liquid crystals. The temperature dependence of λ (coupling to ϕ_1) and β (coupling to ϕ_2) is complex but consistent across nematogens. Within 5 K of T_{NI}, the coupling to ϕ_2 increases dramatically, possibly indicative of the effect of growing long-range orientational correlation. The dramatic shift in the behavior of λ and β matches the temperature at which deviation of spectral diffusion time constants between liquid crystals and a nonmesogenic liquid was first observed.[23,24] Thus, the model for ϕ_3, based on coupling to ϕ_1 and ϕ_2, is capable of tracking these complex dynamics.

It is often the case that the source of spectral diffusion can only be determined through full MD simulations of the system. Modeling the 2D IR data as some combination of coupling to both density and orientational fluctuations using ϕ_3 requires only another set of experiments, namely, OHD-OKE spectroscopy. A similar procedure may be possible for a wide variety of other liquids studied with 2D IR, as OHD-OKE is a nonresonant technique only requiring some anisotropic polarizability to obtain the signal.

The applicability of our ϕ_3 model to other liquids has not been thoroughly explored. Initial attempts to fit spectral diffusion data for the nonmesogenic liquid 5B using an MCT equation for ϕ_3 that contains coupling only to ϕ_1 were not successful. Thus, the spectral diffusion and its temperature dependence in the normal liquid cannot be due only to proximity to the mode-coupling temperature. Including coupling to ϕ_2 in the memory function, as in eq 11, drastically improves the fit of ϕ_3 to 2D IR data, but the quality is not as good as observed for liquid crystals. One possible explanation is that, in a nematogen, the approach to the critical point has such a strong effect on the FFCF that the memory function in eq 11 is adequate to describe the longest time decay of the FFCF but that in a normal liquid, when it is not supercooled, coupling to additional variables may be required to obtain an adequate description.

Finally, we proposed that the temperature dependence of the 2D IR spectral diffusion data arises from small wave vector (long wavelength) density fluctuations that undergo critical slowing as T_{NI} is approached from above. It is worth reviewing the information obtained from previous experiments that leads to the conclusion that small wave vector density fluctuations are responsible for the spectral diffusion.[23] The orientational relaxation measured with the OHD-OKE experiments is orders of magnitude slower than spectral diffusion (CLS(T_w) decay) at all temperatures. The MCT calculations of the OHD-OKE results yield the orientational correlation function, and then, the derivative is taken to compare to the data (see red dashed curve in Figure 1B). At high temperature, where the slowest spectral diffusion component is ~100 ps, the decay of the orientational correlation function occurs in tens of nanoseconds. At low temperature, near the phase transition, the slowest component of the spectral diffusion is ~1 ns, while the long time decay of the orientational correlation function is ~1 μs. Over the entire time scale of the CLS(T_w) decay to zero, the orientational correlation function decays a few percent. Therefore, orientational relaxation of the pseudonematic domains is far too slow to account for the spectral diffusion. In addition, orientation relaxation measurements using polarization selective IR pump–probe experiments of the vibrational probe 5SeCB show zero orientational relaxation within experimental error over the time scale of the spectral diffusion. Therefore, neither the orientational motions of the nematogens nor those of the vibrational probe contribute to the observed spectral diffusion.

It is interesting to note that these results demonstrate that orientation variations do not contribute to the inhomogeneous broadening of the CN stretch of 5SeCB in the nematogens. The CLS(T_w) decays to zero, which means that all structures that contribute to inhomogeneous broadening have been sampled. If orientations contributed a portion of the inhomogeneous broadening, then the CLS would decay to a constant value on the experimentally accessible time scale, not to zero. The lack of orientational contributions to inhomogeneous broadening is likely due to the local ordering of the pseudonematic domains. Small local differences in orientational structure that influence the frequency can be sampled very fast so that they are motionally narrowed and contribute to the homogeneous broadening rather than inhomogeneous broadening of the absorption spectrum.

If the cause of spectral diffusion is not orientational fluctuations, that leaves density fluctuations. The large wave vector density correlation function, ϕ_1, is obtained from fitting the OHD-OKE data. In contrast to the orientational relaxation, ϕ_1 decays in hundreds of picoseconds, which is approximately the time scale of the spectral diffusion. However, the functional form of the ϕ_1 decay is vastly different from the measured CLS(T_w) decay (spectral diffusion), and ϕ_1 is temperature independent in the fits to the OHD-OKE data over the temperature range studied. Allowing the parameters in ϕ_1 to vary with temperature in fitting the OHD-OKE data did not improve the fits, and the parameters changed <10% and not systematically as the temperature was lowered. This is in contrast to the temperature dependence of ϕ_1 parameters for supercooled liquids as the MCT transition temperature is approached.[19,20] ϕ_1 is the large wave vector, essentially single particle, density correlation function.[42] With orientational fluctuations and very local density fluctuations ruled out as

DOI: 10.1021/acs.jpcb.6b04997
J. Phys. Chem. B 2016, 120, 7003–7015

the source of spectral diffusion, that leaves small wave vector (long wavelength) density fluctuations responsible for the spectral diffusion. The divergence of the spectral diffusion time constants approaching the isotropic to nematic phase transition goes as $[T^*/(T - T^*)]^{1/2}$, which is the same temperature dependence as the correlation length of the pseudonematic domains (see eq 1), and very different from the divergence of the orientational relaxation times (see eq 2). In rough analogy to the correlation length growth and critical slowing of density fluctuations in supercritical fluids as the critical point is approached from above, the picture that emerges for dynamics that give rise to spectral diffusion in the isotropic phase of liquid crystals is that there is a density correlation length that grows and the density fluctuations undergo critical slowing as T_{NI} is approached from above.

AUTHOR INFORMATION

Corresponding Author

*E-mail: fayer@stanford.edu.

Notes

The authors declare no competing financial interest.

ACKNOWLEDGMENTS

This work was funded by the Division of Chemistry, Directorate of Mathematical and Physical Sciences, National Science Foundation (NSF) Grant No. CHE-1461477. K.P.S. thanks ARCS for fellowship support.

REFERENCES

(1) deGennes, P. G.; Prost, J. *The Physics of Liquid Crystals*; Clarendon Press: Oxford, United Kingdom, 1974.

(2) Sinha, A.; Prasada Rao, T. A.; Dabrowski, R. Transient Electro-Optic Kerr Effect in Liquid Crystalline Isothiocyanates. *J. Phys. Soc. Jpn.* **1999**, *68* (6), 1939−1942.

(3) Carbone, G.; Barberi, R. Atomic Force Microscope Study of Presmectic Modulation in the Nematic and Isotropic Phases of the Liquid Crystal Octylcyanobiphenyl Using Piezoresistive Force Detection. *Phys. Rev. E: Stat. Phys., Plasmas, Fluids* **2005**, *71*, 051704.

(4) Krich, J. J.; Romanowsky, M. B.; Collings, P. J. Correlation Length and Chirality of the Fluctuations in the Isotropic Phase of Nematic and Cholesteric Liquid Crystals. *Phys. Rev. E: Stat. Phys., Plasmas, Fluids* **2005**, *71*, 051712.

(5) Gierke, T. D.; Flygare, W. H. Depolarized Rayleigh Scattering in Liquids. Molecular Reorientation and Orientation Pair Correlations in a Nematic Liquid Crystal: MBBA. *J. Chem. Phys.* **1974**, *61*, 2231−2239.

(6) Litster, J. D. Critical Slowing of Fluctuations in a Nematic Liquid Crystal. *J. Appl. Phys.* **1970**, *41*, 996−997.

(7) Štěpáanek, P.; Sedláček, B. Investigation of Dynamic Light Scattering in a Nematic Liquid Crystal. *J. Polym. Sci., Polym. Symp.* **1977**, *61*, 123−128.

(8) Dodge, M. R.; Petschek, R. G.; Rosenblatt, C. Light Scattering Investigation above the Nematic-Smectic-A Phase Transition in Binary Mixtures of Calamitic and Bent-Core Mesogens. *Phys. Rev. E: Stat. Phys., Plasmas, Fluids, Relat. Interdiscip. Top.* **2003**, *68*, 031703.

(9) Stankus, J. J.; Torre, R.; Marshall, C. D.; Greenfield, S. R.; Sengupta, A.; Tokmakoff, A.; Fayer, M. D. Nanosecond Time Scale Dynamics of Pseudo-Nematic Domains in the Isotropic Phase of Liquid Crystals. *Chem. Phys. Lett.* **1992**, *194*, 213−216.

(10) Gottke, S. D.; Cang, H.; Bagchi, B.; Fayer, M. D. Comparison of the Ultrafast to Slow Time Scale Dynamics of Three Liquid Crystals in the Isotropic Phase. *J. Chem. Phys.* **2002**, *116*, 6339−6347.

(11) Cang, H.; Li, J.; Fayer, M. D. Short Time Dynamics in the Isotropic Phase of Liquid Crystals: The Aspect Ratio and the Power Law Decay. *Chem. Phys. Lett.* **2002**, *366*, 82−87.

(12) Cang, H.; Li, J.; Novikov, V. N.; Fayer, M. D. Dynamics in Supercooled Liquids and in the Isotropic Phase of Liquid Crystals: A Comparison. *J. Chem. Phys.* **2003**, *118*, 9303−9311.

(13) Cang, H.; Li, J.; Novikov, V. N.; Fayer, M. D. Dynamical Signature of Two "Ideal Glass Transitions" in Nematic Liquid Crystals. *J. Chem. Phys.* **2003**, *119* (19), 10421−10427.

(14) Poggi, Y.; Fillippini, J. C. Magnetic-Field Dependence of the Order Parameter in a Nematic Single Crystal. *Phys. Rev. Lett.* **1977**, *39*, 150−152.

(15) McMorrow, D.; Lotshaw, W. T. Intermolecular Dynamics in Acetonitrile Probed with Femtosecond Fourier Transform Raman Spectroscopy. *J. Phys. Chem.* **1991**, *95* (25), 10395−10406.

(16) McMorrow, D.; Lotshaw, W. T.; Kenney-Wallace, G. A. Femtosecond Optical Kerr Studies on the Origin of the Nonlinear Response in Simple Liquids. *IEEE J. Quantum Electron.* **1988**, *24*, 443−454.

(17) Li, J.; Cang, H.; Anderson, H. C.; Fayer, M. D. A Mode Coupling Theory Description of the Short and Long-Time Dynamics of Nematogens in the Isotropic Phase. *J. Chem. Phys.* **2006**, *124*, 014902.

(18) Sjögren, L. Diffusion of Impurities in a Dense Fluid near the Glass Transition. *Phys. Rev. A: At., Mol., Opt. Phys.* **1986**, *33*, 1254−1260.

(19) Götze, W.; Sperl, M. Nearly Logarithmic Decay of Correlations in Glass-Forming Liquids. *Phys. Rev. Lett.* **2004**, *92*, 105701.

(20) Li, J.; Cang, H.; Andersen, H. C.; Fayer, M. D. The Boson Peak in Supercooled Liquids: Time Domain Observations and Mode Coupling Theory. *J. Chem. Phys.* **2006**, *124*, 014902.

(21) Reddy, R. R.; Venkatesulu, A.; Rama Gopal, K.; Neelakanteswara Reddy, K. Thermo Acoustic Parameters in the Nematic and Isotropic Phases of 5CB and Tetraethyl Methane in 5CB. *J. Mol. Liq.* **2007**, *130*, 112−118.

(22) Oweimreen, G. A.; Shihab, A. K.; Halhouli, K.; Sikander, S. F. Density Measurements in the Nematic and Isotropic Phases of 5Cb and Dilute Solutions of Tetraethylmethane in 5CB. *Mol. Cryst. Liq. Cryst.* **1986**, *138*, 327−338.

(23) Sokolowsky, K. P.; Bailey, H. E.; Fayer, M. D. Length Scales and Structural Dynamics in Nematogen Pseudonematic Domains Measured with 2D IR Vibrational Echoes and Optical Kerr Effect Experiments. *J. Phys. Chem. B* **2014**, *118*, 7856−7868.

(24) Sokolowsky, K. P.; Bailey, H. E.; Fayer, M. D. New Divergent Dynamics in the Isotropic to Nematic Phase Transition of Liquid Crystals Measured with 2D IR Vibrational Echo Spectroscopy. *J. Chem. Phys.* **2014**, *141*, 194502.

(25) Sokolowsky, K. P.; Fayer, M. D. Dynamics in the Isotropic Phase of Nematogens Using 2D IR Vibrational Echo Measurements on Natural Abundance ^{13}CN and Extended Lifetime Probes. *J. Phys. Chem. B* **2013**, *117*, 15060−15071.

(26) Sturlaugson, A. L.; Fruchey, K. S.; Fayer, M. D. Orientational Dynamics of Room Temperature Ionic Liquid/Water Mixtures: Evidence for Water-Induced Structure and Anisotropic Cation Solvation. *J. Phys. Chem. B* **2012**, *116*, 1777−1787.

(27) Smith, N. A.; Meech, S. R. Optically-Heterodyne-Detected Optical Kerr Effect (OHD-OKE): Applications in Condensed Phase Dynamics. *Int. Rev. Phys. Chem.* **2002**, *21*, 75−100.

(28) Kinoshita, S.; Sakai, Y.; Miyazaki, J.; Watanabe, J. Fundamental Aspects of Light Scattering and Optical Kerr Effect Spectroscopy. *Eur. Phys. J.: Spec. Top.* **2012**, *209*, 1−100.

(29) Sturlaugson, A. L.; Arima, A. Y.; Bailey, H. E.; Fayer, M. D. Orientational Dynamics in a Lyotropic Room Temperature Ionic Liquid. *J. Phys. Chem. B* **2013**, *117*, 14775−14784.

(30) Nicolau, B. G.; Sturlaugson, A.; Fruchey, K.; Ribeiro, M. C. C.; Fayer, M. D. Room Temperature Ionic Liquid-Lithium Salt Mixtures: Optical Kerr Effect Dynamical Measurements. *J. Phys. Chem. B* **2010**, *114* (25), 8350−8356.

(31) Sturlaugson, A. L.; Fruchey, K. S.; Lynch, S. R.; Aragon, S. R.; Fayer, M. D. Orientational and Translational Dynamics of Polyether/Water Solutions. *J. Phys. Chem. B* **2010**, *114*, 5350−5358.

DOI: 10.1021/acs.jpcb.6b04997
J. Phys. Chem. B 2016, 120, 7003−7015

(32) Cang, H.; Novikov, V. N.; Fayer, M. D. Logarithmic Decay of the Orientational Correlation Function in Supercooled Liquids on the Ps to Ns Time Scale. *J. Chem. Phys.* **2003**, *118*, 2800−2807.
(33) Li, J.; Wang, I.; Fayer, M. D. Ultrafast to Slow Orientational Dynamics of a Homeotropically Aligned Nematic Liquid Crystal. *J. Phys. Chem. B* **2005**, *109*, 6514−6519.
(34) Li, J.; Wang, I.; Fayer, M. D. Three Homeotropically Aligned Nematic Liquid Crystals: Comparixon of Ultrafast to Slow Time-Scale Dynamics. *J. Chem. Phys.* **2006**, *124*, 044906.
(35) Park, S.; Kwak, K.; Fayer, M. D. Ultrafast 2D-IR Vibrational Echo Spectroscopy: A Probe of Molecular Dynamics. *Laser Phys. Lett.* **2007**, *4*, 704−718.
(36) Zheng, J.; Kwak, K.; Fayer, M. D. Ultrafast 2D IR Vibrational Echo Spectroscopy. *Acc. Chem. Res.* **2007**, *40*, 75−83.
(37) Mukamel, S. *Principles of Nonlinear Optical Spectroscopy*.; Oxford University Press: New York, 1995.
(38) Mukamel, S. Multidimensional Femtosecond Correlation Spectroscopies of Electronic and Vibrational Excitations. *Annu. Rev. Phys. Chem.* **2000**, *51*, 691−729.
(39) Kubo, R. A Stochastic Theory of Line-Shape and Relaxation. In *Fluctuation, Relaxation and Resonance in Magnetic Systems*; Ter Haar, D., Ed.; Oliver and Boyd: London, 1961.
(40) Kwak, K.; Park, S.; Finkelstein, I. J.; Fayer, M. D. Frequency-Frequency Correlation Functions and Apodization in 2D-IR Vibrational Echo Spectroscopy, a New Approach. *J. Chem. Phys.* **2007**, *127*, 124503.
(41) Kwak, K.; Rosenfeld, D. E.; Fayer, M. D. Taking Apart the Two-Dimensional Infrared Vibrational Echo Spectra: More Information and Elimination of Distortions. *J. Chem. Phys.* **2008**, *128*, 204505.
(42) Götze, W. *Liquids, Freezing and Glass Transition*; Elsevier Science Publishers: Amsterdam, The Netherlands, 1989.
(43) Sciortino, F. Slow Dynamics in Supercooled Water. *Chem. Phys.* **2000**, *258*, 307−314.
(44) Cummins, H. Z.; Li, G.; Du, W. M.; Hernandez, J.; Tao, N. J. Depolarized Light Scattering Spectroscopy of Glassforming Liquids: Experimental Tests of MCT. *Transp. Theory Stat. Phys.* **1995**, *24*, 981−1016.
(45) Bartsch, E.; Fujara, F.; Geil, B.; Kiebel, M.; Petry, W.; Schnauss, W.; Sillescu, H.; Wuttke, J. Signatures of the Glass Transition in a Van Der Waals Liquid Seen by Neutrons and NMR. *Phys. A* **1993**, *201*, 223−236.
(46) Jadzyn, J.; Czechowski, G.; Lech, T. Temperature Dependence of the Viscosity of Isotropic Liquids. *Acta Phys. Pol., A* **2002**, *101*, 495−503.
(47) Kuss, E. The Viscosity-Pressure Behavior of Three 4-Trans-(4-Alkyl)-Cyclohexyl-Benzonitriles and of an Eutectic Mixture. *Mol. Cryst. Liq. Cryst.* **1983**, *91*, 59−76.
(48) Eidenschink, R.; Erdmann, D.; Krause, G.; Pohl, L. Substituted Phenylcyclohexanes - a New Class of Liquid Crystalline Compounds. *Angew. Chem., Int. Ed. Engl.* **1977**, *16*, 100.
(49) Pohl, L.; Eidenschink, R.; Krause, G.; Erdmann, D. Physical Properties of Nematic Phenylcyclohexanes, a New Class of Low Melthing Liquid Crystals with Positive Dielectric Anisotropy. *Phys. Lett. A* **1977**, *60*, 421−423.
(50) Simeão, D. S.; Simões, M. Universality of the Nematic Mesophase. *Phys. Rev. E: Stat. Phys., Plasmas, Fluids* **2012**, *86*, 042701.
(51) Schweizer, K. S.; Chandler, D. Vibrational Dephasing and Frequency Shifts of Polyatomic Molecules in Solution. *J. Chem. Phys.* **1982**, *76*, 2296−2314.

DOI: 10.1021/acs.jpcb.6b04997
J. Phys. Chem. B 2016, 120, 7003−7015